Enabling the Prediction of Manoeuvring Characteristics of a Submarine Operating Near the Free Surface

C Polis[1], D Ranmuthugala[1], J Duffy[1], M Renilson[1,2]
1. Australian Maritime College, 2. Higher Colleges of Technology, UAE

ABSTRACT

Predicting the behaviour of a submarine operating close to the free surface is important in order to assess the merits of particular designs, identify the operational characteristics, and determine a safe operating envelope. To predict submarine behaviour near the free surface requires both a mathematical model that captures the dynamics of a submarine in motion, and an understanding of the additional forces and moments generated in the near surface region. In the past, submarine manoeuvring models in published literature have neglected the effect of the presence of the free surface, thus the authors are developing a coefficient based submarine manoeuvring model incorporating the effects of near surface operation. The hydrodynamic coefficients required for the model are obtained using Computational Fluid Dynamics (CFD) and validated against results from captive model experiments in the Australian Maritime College (AMC) towing tank. This paper describes hydrodynamic coefficients that can be added to existing submarine manoeuvring models to account for near surface effects in the vertical plane, for the SUBOFF geometry. Validated CFD predictions of the forces acting on a generic submarine operating near the free surface are presented along with empirically based equations to predict them.

1. INTRODUCTION

It is important to be able predict the behaviour of a submarine operating close to the free surface in order to determine its operational characteristics, improve the response of control systems, and develop procedures and limitations for safe operation. This requires both a mathematical model that captures the dynamics of the submarine in motion and an understanding of the additional forces generated in the near surface region. In the past a number of researchers have developed mathematical models to describe deeply submerged submarine motion, capturing the characteristics thereof in manoeuvring coefficients within equations of motion (Feldman, 1979 and Gertler & Hagen, 1967). The work included the prediction of the relevant manoeuvring coefficients through experimental and numerical procedures.

However, these manoeuvring models neglect the effect of the free surface, as they represent vehicles operating deep enough in the water such that there is no significant influence from the free surface. This is not to indicate that these effects have been completely ignored, with researchers such as Lamb (1926) and Havelock (1928) extending potential flow theory to allow the prediction of wave resistance of submerged objects and Weinblum (1936) conducting captive model tests to investigate the wave resistance of submarine like bodies of revolution. The development of numerical methods and computational capability over the last three decades has enabled the prediction of the coefficients of motion for different hull forms at various water depths and speeds, with the work of Griffin (2002) and Renilson & Ranmuthugala (2012) being recent examples.

This paper examines the additional forces acting on an un-appended SUBOFF geometry submarine (Groves et al. 1989) travelling in a steady-state level operating condition near the free surface, with a view to extending the existing standardised equations of motion to incorporate free surface effects. As part of an on-going project to develop a model of submarine motion inclusive of near surface effects, numerical estimates of the coefficients obtained from Computational Fluid Dynamics (CFD) studies are validated herein against captive model tests results, and expressed as a continuous mathematical function. As this model is developed, it will inform design and operational procedures, including refining the limitations for safe operation when close to the free surface.

2. REPRESENTATION OF THE FORCES ACTING ON A SUBMARINE TRAVELLING NEAR THE FREE SURFACE

The depth of submergence of the submarine is represented by $H^{\star}$, which is defined as the ratio of the submergence of the submarine longitudinal centreline to the hull diameter (i.e. $H^{\star} = H/D$). The parameters used to define the submergence, and the coordinate system are shown in Figure 1.

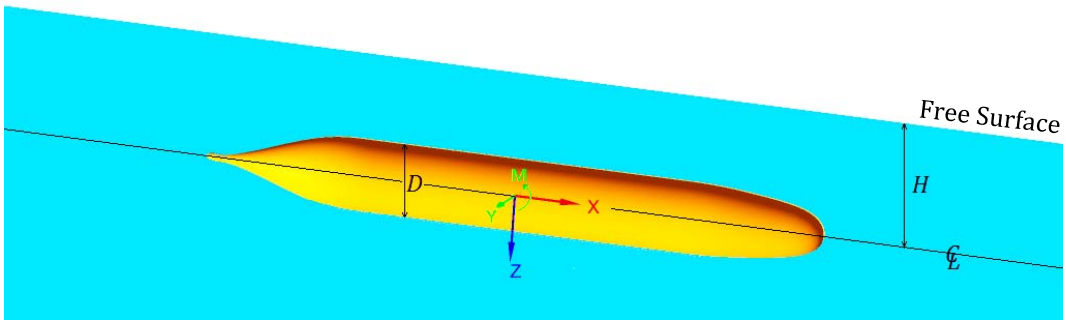

Figure 1 – SUBOFF Orientation Showing Submergence and Coordinate System

When operating close to the free surface under level, steady-state conditions, forces act on a submarine that are dependent on the speed and the submergence. The changes to the surge and heave forces, and to the pitch moment, for a submarine operating near the free surface are functions of the Froude number rather than the Reynolds number as is the case for submarines operating deeply submerged. This is because the surface effects are dominated by wave making rather than friction. Hence, forces will be presented as a function of Froude number.

Existing submarine manoeuvring models, such as the Feldman (1979) model, require the forces acting on the submarine to be known in order to determine its path. This model can be extended to predict the path of a submarine operating near the free surface by including the forces and moments acting on the submarine under such conditions. As near surface effects primarily occur in the vertical plane, and it is motions in the vertical plane that will affect the safe operating envelope, the effects of sway, roll, and yaw have been neglected in the present work. Under level, steady-state conditions, with the control plane angles set to zero, the forces and moments instantaneously acting upon the submarine can be captured considering solely the terms representing the forward velocity of the submarine due to its asymmetry. These terms in the Feldman equations, describing motion for a deeply submerged submarine, are $[(a_i + \Delta X)u^2 + b_i C u u_c + c_i C^2 u_c^2]$ in surge, $Z_{\star}u^2$ in heave and $M_{\star}u^2$ in pitch. In the surge term, the a_i, b_i and c_i constants capture the thrust and drag relationship between vessel

speed (u) and command speed (u_c); ΔX corrects the model test data results to full scale. For consistency with the other axes, we define $X_\star$ such that:

$$X_\star u^2 = (a_i + \Delta X)u^2 + b_i C u u_c + c_i C^2 u_c^2 \quad (1)$$

To extend the use of the coefficients $X_\star$, $Z_\star$ and $M_\star$ to capture the near surface effects, we herein express these in non-dimensional form as a function of Froude number and submergence.

$$X'_\star(Fr, H^\star) = X'_{\star ds} + \Delta X'_\star(Fr, H^\star) \quad (2)$$

$$Z'_\star(Fr, H^\star) = Z'_{\star ds} + \Delta Z'_\star(Fr, H^\star) \quad (3)$$

$$M'_\star(Fr, H^\star) = M'_{\star ds} + \Delta M'_\star(Fr, H^\star) \quad (4)$$

where $X'_{\star ds}$, $Z'_{\star ds}$ and $M'_{\star ds}$ represent the non-dimensional coefficients for the deeply submerged case, and the terms $\Delta X'_\star(Fr, H^\star)$, $\Delta Z'_\star(Fr, H^\star)$ and $\Delta M'_\star(Fr, H^\star)$ represent the additional non-dimensional forces and moments due to the influence of the nearby free surface. For reference, the non-dimensionalisation formulae used are provided in the nomenclature at the end of this paper.

3. NUMERICAL ANALYSIS OF THE FORCES ON A SUBMARINE TRAVELLING NEAR THE FREE SURFACE

3.1 CFD Modelling

ANSYS CFX was used to model the standard un-appended SUBOFF model running straight and level in open water near the free surface, to predict the hydrodynamic surge force, heave force and pitch moment acting on the submarine. The CFD domain geometry utilised is shown in Figure 2(a) viewed from the longitudinal vertical symmetry plane, with the bow of the model towards the right. The entire domain modelled extends over three lengths forward of the bow of the boat and four lengths to the side of the centreline, in order to provide sufficient damping of the wave train to minimise boundary effects. The distance modelled aft is dependant on the speed of the submarine to allow resolution of the longer wavelengths generated at higher speeds, while limiting the scale of the geometry for lower speeds as solution time is highly dependent on the number of wavelengths modelled. A body of influence defining the region in which the wave train is to be modelled is shown as the "Wave Resolution Region" in Fig 2(a), with a wake region defined behind the submarine hull. A free surface layer is produced as a distinct part of the geometry between the air and water regions.

Figure 2(b) shows the unstructured mesh used to map the space around the submarine. Using unstructured mesh requires a higher cell count for the same accuracy, with correspondingly longer calculation times but significantly less design time. The choice to use unstructured mesh here is a provision for future work as the current submarine form can be replaced with any submarine geometry without having to redevelop a structured mesh. The free surface layer forms a clearly distinct part of the mesh. This layer is relatively thin and composed of high aspect ratio prismatic cells, reflective of the ratio of wave height to wave length. An inflation layer expands gradually away from the free surface to either side, until the cells achieved acceptable proportions.

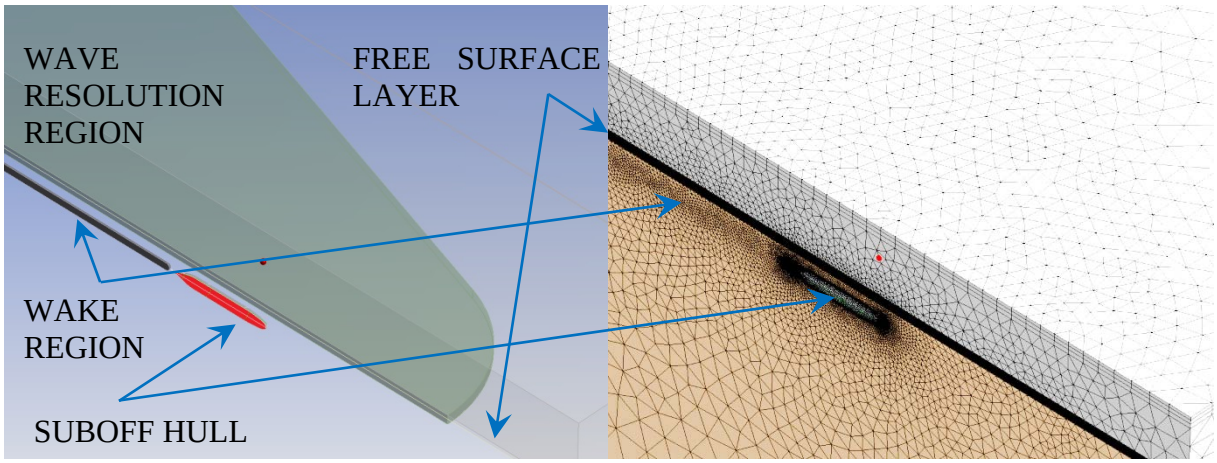

Figure 2 - (a) CFD Geometry; (b) Mesh Domain

A no slip boundary condition was set for the hull. An inlet condition was applied to the upstream face, specifying the water / air proportions and velocity. Entrainment openings were used elsewhere, with a static pressure distribution specified to match the hydrostatic pressure. A symmetry condition was used in the vertical plane as the flow is symmetric in these cases. All simulations were carried out with the Shear Stress Transport (SST) turbulence model, as it is known to provide accurate results for steady-state conditions at low angles of incidence. (Renilson & Ranmuthugala, 2012). While potential flow methods could have been utilised for this work without significant loss of accuracy (Tuck and Scullen, 2002), considerations of future studies including fully appended models and different test conditions influenced the decision to utilise the more time intensive approach.

Using these meshes, CFD simulations were run for the speed range from Fr = 0.340 to Fr = 0.500, and at submergences ($H^{\star}$) of 1.8, 2.2, 2.5, and 2.8. This corresponds to speeds of 18.5 to 27 knots for an 80m submarine at depths approaching snorkelling depth. These cases were repeated with the same mesh and conditions, however without the free surface, thus calculating the equivalent deeply submerged condition for comparison.

A series of tests were conducted to ascertain the grid independence of the mesh arrangement utilised. These included: assessment of the mesh density required to produce consistent pressure results on the surface of the submarine (both in terms of the mesh density required at various points along the vessel and assessment of the required inflation layer arrangement); assessment of free surface response in waves generation above the hull; and assessment of the wake field downstream of the hull. The requirements for local mesh density on the surface of the submarine were assessed utilising a process of mesh adaption. Starting with a coarse mesh, ANSYS CFX iteratively increased the density of the mesh in areas where this was lacking resolution relative to rate of change of specified properties (such as pressure, velocity and sheer strain rate) in the fluid.

Figure 3(a) shows the effect on the surge, heave and pitch coefficients as the mesh layer thickness adjacent to the hull is increased, i.e. y^{+} is increased. For the heave and pitch coefficients, the independence of the coefficients falls away as the y^{+} value exceeds 2, although for surge the effect remains small well beyond this value. These results are in line with the recommendations for the SST turbulence model, which requires a y^{+} value below 1 to provide accurate lift forces and moments, but is able to provide drag results at low angles of incidence up to around a y^{+} value of 8.

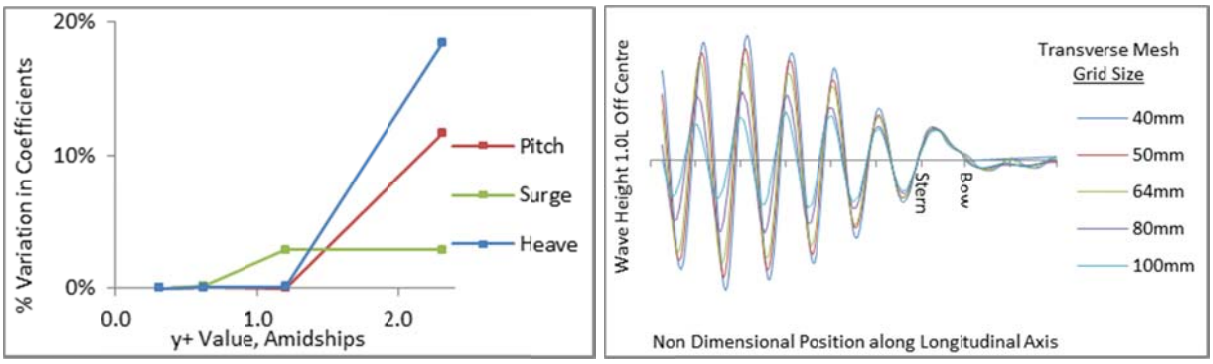

Figure 3 – (a) % Variation of Coefficients with y+ (b); Variation in Surface Waves due to Change in Free Surface Transverse Mesh Size

Figure 3(b) shows the propagation and definition of the surface wave due to the submarine hull operating close to the surface for different mesh densities on the hull surface, clearly showing the dependence of adequate mesh densities. Below a certain density, the resultant reduction in wave height will adversely affect the pressure and friction forces on the hull and thus the estimation of the hydrodynamic coefficients. It was also important from a stability and accuracy point of view, especially at low Froude numbers, to provide damping around the wake zone. The ripple produced as a result of the initial formation of the wake will escalate in height if the artificial time step is too high (Polis et al, 2013). These ripples can travel at a wave speed slightly faster than the boat and produce a continuing oscillation in the forces experienced by the hull. Although these ripples are small, at lower Froude numbers they are significant in comparison to the wave train. This is addressed by maintaining the free surface mesh in the Wave Resolution Region (see Figure 2(a)) of sufficient density to capture the waves based on the wave length, while further afield the mesh size is increased to absorb and dampen out the wave energy near the boundaries.

3.2 Validation

Comparative CFD and experimental work at AMC (Leong, 2013 and Neulist, 2011 as cited in Polis et al, 2013) has been used to validate the CFD results presented herein. The AMC has a 1.556m long SUBOFF model which has been used to examine hydrodynamic characteristics, including near surface effects, in captive model testing within AMC's towing tank. The model is secured to a Horizontal Planar Motion Mechanism (HPMM) using a vertical strut and a stern entry sting that supports an internal force balance as shown in Figure 4.

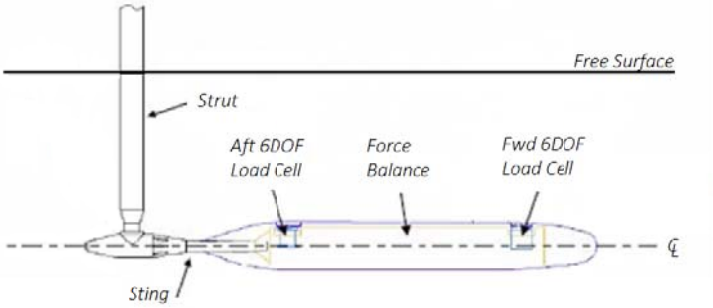

Figure 4 - SUBOFF Model Showing Mounting Arrangement

The effects of the HPMM mounting strut and sting upon the resistance recorded at different depths and speeds (see Figure 5) were modelled numerically, thus enabling the CFD models herein to be validated against this comparative data. Figure 5 shows that the coefficient of drag (C_D) of the CFD model developed for this study is in good agreement with that of the model previously validated.

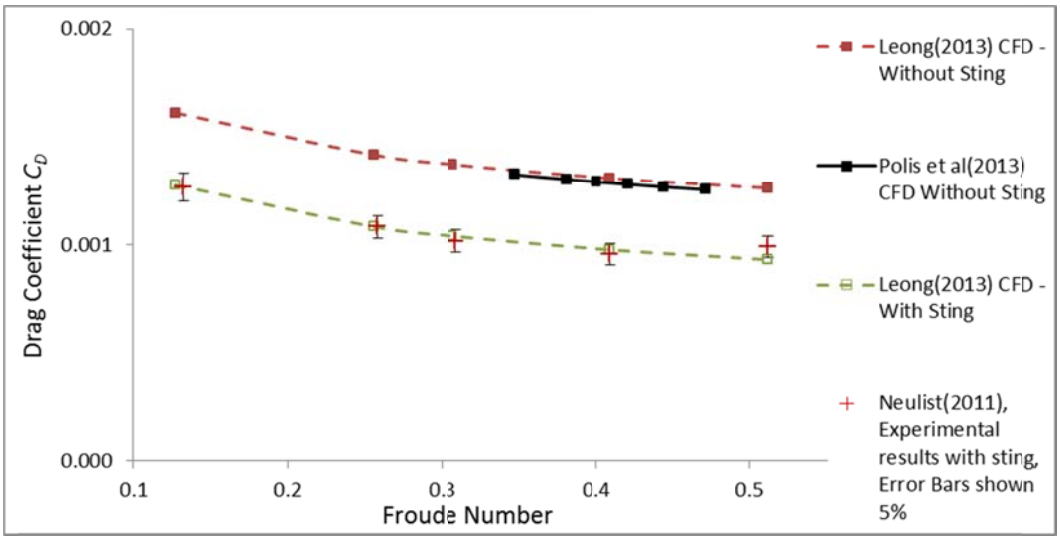

Figure 5 - Comparison of CFD and Experimental Results for the Deep Case

4. RESULTS

4.1 Influence of Submergence on Surge, Heave and Pitch

Figures 6, 7, and 8 present the changes in the free surface induced hydrodynamic coefficients (surge, heave, and pitch) as the submarine speed and submergence are varied. Note that the values presented are $\Delta X'_{\star}(Fr, H^{\star})$, $\Delta Z'_{\star}(Fr, H^{\star})$, and $\Delta M'_{\star}(Fr, H^{\star})$ as noted in equations (5), (6) and (7), i.e. the coefficients of the additional forces and moments due to the free surface, obtained from the difference between the CFD simulations near the free surface and a deeply submerged case. They correspond to steady-state, straight and level conditions and all unsteady terms are excluded. Furthermore these results are for an un-appended submarine hull, and it is possible that the interaction of a submarine sail with the surface will alter the nature of the decay rates of these curves.

In Figure 6 the surge coefficient increases with the Froude number. There is a marked decrease in the magnitude of $\Delta X'_{\star}(Fr, H^{\star})$ with increasing submergence. Figure 7 shows $\Delta Z'_{\star}(Fr, H^{\star})$ peaking at around Fr 0.42 for a submergence of 1.8. Again, there is a marked decrease in magnitude with increasing submergence. From Figure 8 it can be seen that $\Delta M'_{\star}(Fr, H^{\star})$ increases with Fr for all submergences and that there is a marked decrease in the magnitude of the coefficient with increasing submergence.

For comparison, the deeply submerged drag coefficient is between 1.25×10^{-3} and 1.31×10^{-3} within the speed range shown in the charts below.

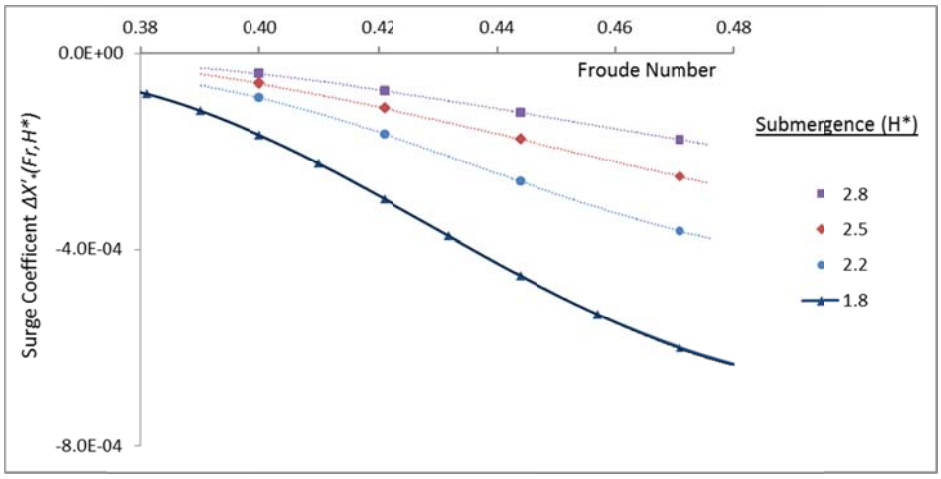

Figure 6 - Surge Coefficient as a Function of Froude Number at Varying Submergence

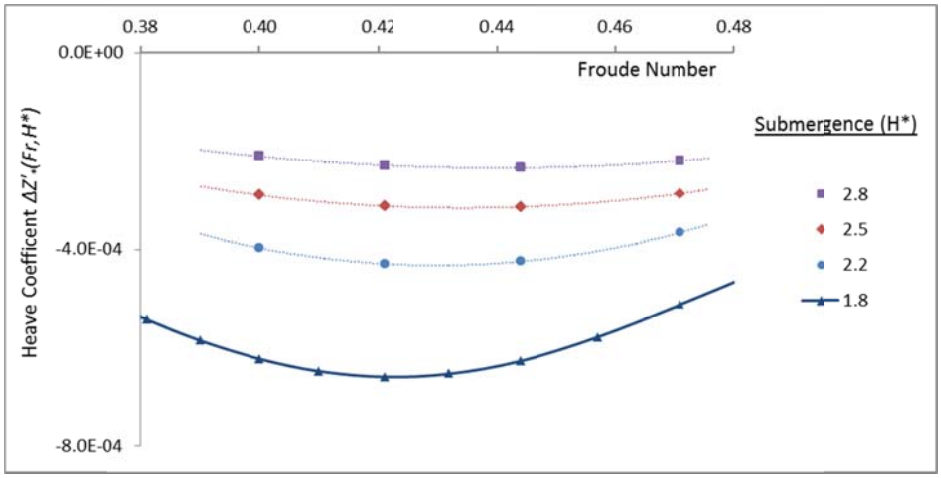

Figure 7 - Heave Coefficient as a Function of Froude Number at Varying Submergence

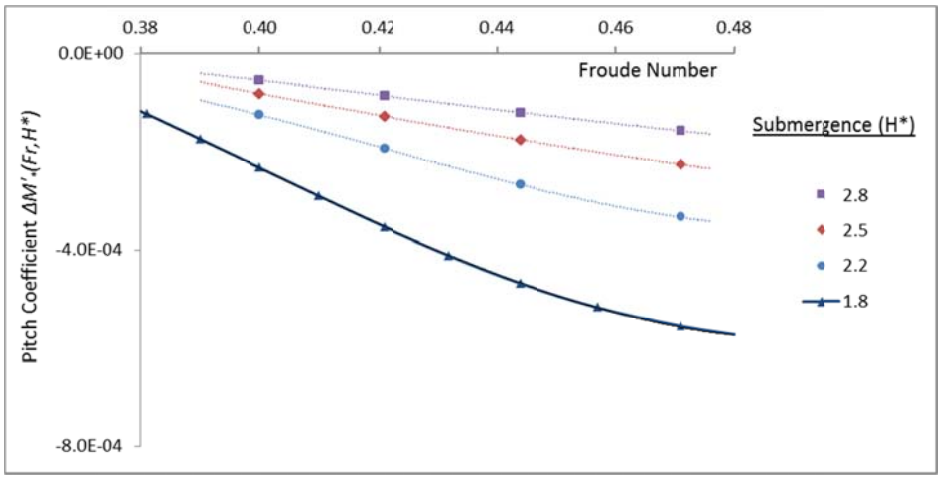

Figure 8 - Pitch Coefficient as a Function of Froude Number at Varying Submergence

Figures 9, 10 and 11 present the log value of the surge, heave and pitch coefficients as a function of the submergence ($H^{\star}$), for different Fr. From these figures it can be seen that the rate of decrease of the coefficients with submergence is reasonably consistent for each Fr. It

should be noted that in Figure 10 the curves for Fr = 0.421 and Fr = 0.444 have been omitted for the sake of clarity.

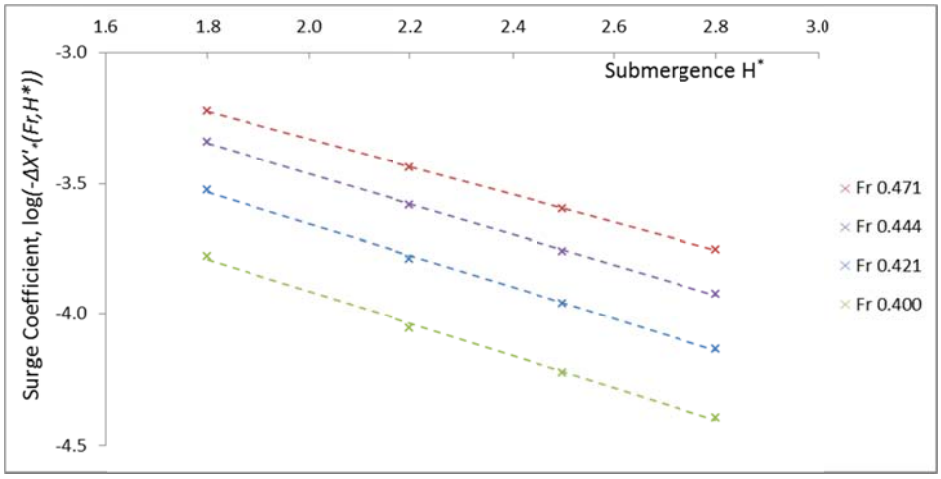

Figure 9 - Surge Coefficient as a Function of Submergence at Varying Froude Number

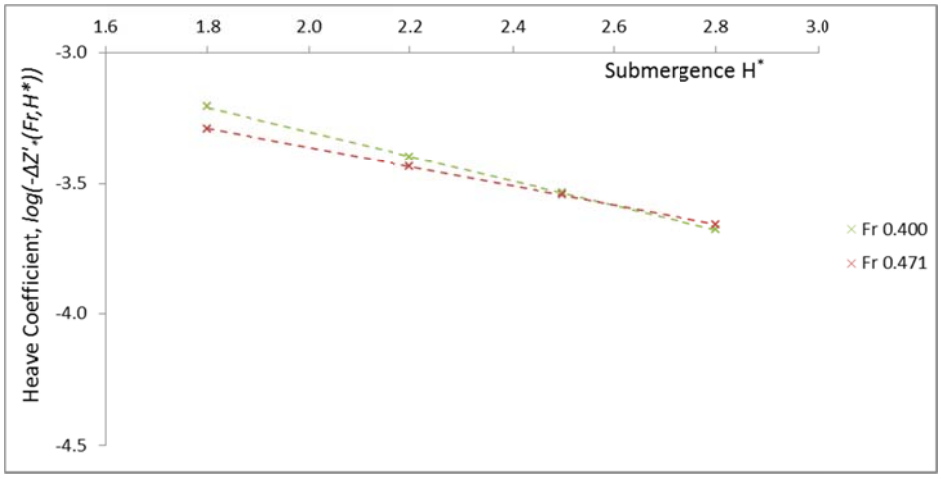

Figure 10 - Heave Coefficient as a Function of Submergence at Varying Froude Number

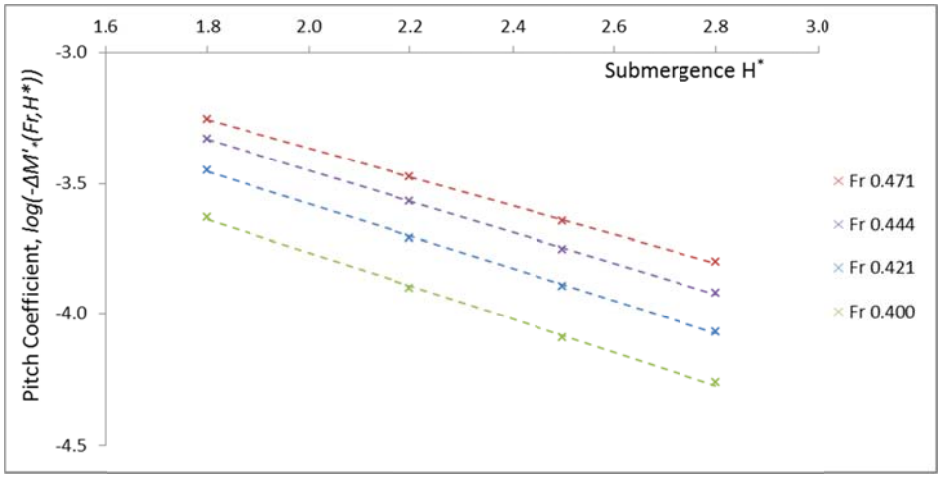

Figure 11 - Pitch Coefficient as a Function of Submergence at Varying Froude Number

4.2 Calculating the Near Surface Coefficients for the SUBOFF geometry

In order to utilise these results within a manoeuvring model, they must be able to be represented mathematically. Figures 9, 10, and 11 clearly show a very close to exponential decay with non dimensional centreline depth ($H^\star$) over the entire range tested. Although the decay rate varies between about 2.0 and 2.7 hull diameters per order of magnitude, it is near constant for each particular speed. Utilising this property, the results that occur between the curves at $H^\star$= 1.8 and $H^\star$ = 2.8 can be expressed as a function of Fr and $H^\star$:

$$X'_\star(H^\star, Fr) = X'_{\star \mathrm{ds}} + \Delta X'_\star(1.8, Fr)\, e^{(H^\star - 1.8)\left(ln\left(\Delta X'_\star(2.8,Fr)\right) - ln\left(\Delta X'_\star(1.8,Fr)\right)\right)} \quad (5)$$

$$Z'_\star(H^\star, Fr) = Z'_{\star \mathrm{ds}} + \Delta Z'_\star(1.8, Fr)\, e^{(H^\star - 1.8)\left(ln\left(\Delta Z'_\star(2.8,Fr)\right) - ln\left(\Delta Z'_\star(1.8,Fr)\right)\right)} \quad (6)$$

$$M'_\star(H^\star, Fr) = M'_{\star \mathrm{ds}} + \Delta M'_\star(1.8, Fr)\, e^{(H^\star - 1.8)\left(ln(\Delta M'_\star(2.8,Fr)) - ln(\Delta M'_\star(1.8,Fr))\right)} \quad (7)$$

If the output of these equations utilising cubic polynomials fitted to the SUBOFF data for $H^\star$ = 1.8 and 2.8, are compared to the results from the CFD for intermediary values, there is a maximum error of 3.4%, and an average error of 1.4%. Thus, testing at the upper bounds of the operational range and the lower bound of consequential effect is all that is necessary to adequately capture these coefficients for the case tested. For larger portions of the speed range an alternative mathematical expression of the curve would be required, or the curve may without significant penalty be broken up into a series of continuous gradient cubic polynomials to cover the entire range required. This formulation allows continuous functions of the additional forces and moments due to the proximity of a free surface to be included within a coefficient based manoeuvring model.

5. CONCLUDING REMARKS

The manoeuvring coefficients within the equations of motion for a submarine travelling near the free surface need to include the effects induced by the free surface. In the current work, hydrodynamic coefficients have been introduced that can be added to existing submarine manoeuvring models to account for near surface effects in the vertical plane. The work presented in this paper quantifies these coefficients for the SUBOFF geometry under steady state, level operation conditions near the free surface. These coefficients were obtained through a study using CFD at varying submergences and speeds, and validated against captive model data, forming an initial basis for understanding the characteristic response of a generic un-appended submarine shape body travelling close to the free surface. The results for different speeds form smooth curves, and the variation with depth in each case can be approximated using an exponential fit. These characteristics allow them to be captured in a relatively simple mathematical expression suited to implementation within a coefficient based manoeuvring model.

The authors are currently extending the model presented here through the selection and assessment of other coefficients that vary near the surface, and to confirm that the formulation of those coefficients holds across a range of submarine like forms, including appended hull forms. A process of assessment is now underway whereby the change in coefficients due to speed and depth are being characterised and their effects on the overall manoeuvring model are identified. As this model develops, it will provide information on design choices, improve control response, and refine the limitations for safe operation when close to the free surface.

6. NOMENCLATURE

a_i, b_i, c_i	Coefficients capturing variation in thrust due to speed and command speed
C	Model to full scale effect coefficient
C_D	Coefficient of drag, $C_D = \frac{Drag}{\frac{1}{2}\rho U^2 L^2}$
D	Diameter of submarine hull in meters
Fr	Froude Number = $u/\sqrt{gL}$
g	Acceleration due to gravity in metres per second squared.
H	Depth from static free surface to the submarine hull centreline in metres
$H^\star$	Submergence, H/D
L	Length of submarine hull in metres
M	Moment about the y-axis; pitching moment
$M_\star u^2$	Component of moment about the y-axis due to forward velocity
$M_\star$	Normalised component of moment about the y-axis due to forward velocity
$M_\star(Fr, H^\star)$	Normalised component of moment proportional to u^2 about the y-axis, incorporating Froude number and submergence related variations
$M'_\star(Fr, H^\star)$	$M'_\star(Fr, H^\star) = \frac{M_\star(Fr,H^\star)\, u^2}{\frac{1}{2}\rho L^3 U^2}$
$\Delta M_\star\ (Fr, H^\star)$	Additional normalised component of moment proportional to u^2 about the y-axis due to forward velocity in proximity to the free surface
$\Delta M'_\star(Fr, H^\star)$	$\Delta M'_\star(Fr, H^\star) = \frac{\Delta M_\star(Fr,H^\star)\, u^2}{\frac{1}{2}\rho L^3 U^2}$
$M_{\star ds}$	Normalised component of moment proportional to u^2 about the y-axis as determined for the deeply submerged case
$M'_{\star \mathrm{ds}}$	$M'_{\star \mathrm{ds}} = \frac{M_{\star ds}(Fr,H^\star)\, u^2}{\frac{1}{2}\rho L^3 U^2}$
U	Vessel speed in metres per second.
u	Component of vessel speed along the x-axis; forward velocity
u_c	Command Speed
x,y,z	Body fixed coordinate axes
X, Z	Force component in the x, z axes; surge and heave
$X_\star u^2, Z_\star u^2$	Component of force in the x,z axes due to forward velocity
$X_\star, Z_\star$	Normalised component of the force in the x,z axes due to forward velocity
$X_\star(Fr, H^\star), Z_\star(Fr, H^\star)$	Normalised component of force in the x,z axes, due to forward velocity incorporating Froude number and submergence related variations
$X'_\star(Fr, H^\star), Z'_\star(Fr, H^\star)$	$X'_\star(Fr, H^\star) = \frac{X_\star(Fr,H^\star)u^2}{\frac{1}{2}\rho L^2 U^2}$, $Z'_\star(Fr, H^\star) = \frac{Z_\star(Fr,H^\star)u^2}{\frac{1}{2}\rho L^2 U^2}$

$X_{\star \mathrm{ds}}, Z_{\star \mathrm{ds}}$	Normalised component of force in the x,z axes due to forward velocity for the deeply submerged case
$X'_{\star \mathrm{ds}}, Z'_{\star ds}$	$X'_{\star \mathrm{ds}} = \frac{(a_i + \Delta X)u^2 + b_i C u u_c + c_i C^2 u_c^2}{\frac{1}{2}\rho L^2 U^2}$, $Z'_{\star ds} = \frac{Z_{\star ds} u^2}{\frac{1}{2}\rho L^2 U^2}$
ΔX	Constant for correcting model scale results to full scale as per Feldman (1979).
$\Delta X_\star(Fr, H^\star), \Delta Z_\star(Fr, H^\star)$	Additional normalised component of force in the x,z axes due to forward velocity in proximity to the free surface.
$\Delta X'_\star(Fr, H^\star), \Delta Z'_\star(Fr, H^\star)$	$\Delta X'_\star(Fr, H^\star) = \frac{\Delta X_\star(Fr, H^\star) u^2}{\frac{1}{2}\rho L^2 U^2}$, $\Delta Z'_\star(Fr, H^\star) = \frac{\Delta Z_\star(Fr, H^\star) u^2}{\frac{1}{2}\rho L^2 U^2}$
ρ	Water density

7. REFERENCES

1. Feldman, J., (1979), "DTNSRDC Revised Standard Submarine Equations of Motion", David Taylor Naval Ship Research and Development Centre, Bethesda
2. Gertler, M. and Hagen, G., (1967), "Standard Equations of Motion for Submarine Simulation", Naval Ship Research and Development Centre, Bethesda
3. Lamb, H., (1926), "On Wave Resistance", Proceedings of the Royal Society of London. Series A, Containing Papers of a Mathematical and Physical Character, Vol. 111, No. 757, pp. 14-25
4. Havelock, T.H., (1928), "Wave Resistance", Proceedings of the Royal Society of London. Series A, Containing Papers of a Mathematical and Physical Character, Vol. 118, No. 779, pp. 24-33
5. Weinblum, G., (1936), "Bodies of Revolution with Minimum Wave Resistance", Ingenieur Archiv VII, p104.
6. Griffin, M.J., (2002), "Numerical Prediction of the Manoeuvring Coefficients of Submarines Operating Near the Free Surface", PhD Thesis, MIT, Massachusetts
7. Renilson, M.R. and Ranmuthugala, D., (2012), "The effect of proximity to free surface on the optimum length/diameter ratio for a submarine", 1st Int Conference on Submarine Technology and Marine Robotics (ICSTaMR 2012), 13 – 14 Jan. 2012, India.
8. Tuck, E.O. and Scullen, D.C. (2002) "A comparison of linear and nonlinear computations of waves made by slender submerged bodies." Journal of Engineering Mathematics 42: 255–264.
9. Groves, N.C., Huang, T.T., and Chang, M.S., (1989), "Geometric Characteristics of DARPA SUBOFF Models", David Taylor Research Centre, Bethesda
10. Roddy, R.F. (1990), "Investigation of the Stability and Control Characteristics of Several Configurations of the DARPA SUBOFF Model From Captive Model Experiments", David Taylor Research Centre, Bethesda
11. Polis, C., Ranmuthugala, D., Duffy, J., and Renilson, M., (2013), "Characterisation of near surface effects acting on an underwater vehicle within the vertical plane", *INEC@IMDEX Asia 2013 Conference*, May 2013, Singapore.